HHS Public Access

Author manuscript

Transplantation. Author manuscript; available in PMC 2022 November 01.

Published in final edited form as:

Transplantation. 2021 November 01; 105(11): e215–e225. doi:10.1097/TP.0000000000003675.

A Novel Multidrug Combination Mitigates Rat Liver Steatosis Through Activating AMPK Pathway During Normothermic Machine Perfusion

Min Xu, MD[1], **Fangyu Zhou, MD**[1], **Ola Ahmed, MD**[1], **Gundumi A. Upadhya, PhD**[1], **Jianluo Jia, MD**[1], **Choonghee Lee, MS**[1], **Jianwei Xing, MS**[1], **Li Ye, MS**[1], **So Hee Shim, PhD**[1], **Zhengyan Zhang, MD, PhD**[1], **Kathleen Byrnes, MD**[2], **Brian Wong, PhD**[1], **Jae-Sung Kim, PhD**[1], **Yiing Lin, MD, PhD**[1], **William C. Chapman, MD**[1]

[1]Department of Surgery, Section of Abdominal Transplantation, Washington University School of Medicine, St. Louis, MO, USA

[2]Department of Pathology and Immunology, Washington University School of Medicine, St. Louis, MO, USA

Abstract

Background: Hepatic steatosis is now the leading cause of liver discards in deceased donors. Previous studies (Y defatting) have successfully reduced the fat content by treating rat steatotic livers on extracorporeal normothermic machine perfusion (NMP) with a multidrug combination including the GW compounds that were linked to an increased risk of carcinogenesis.

Methods: We developed a novel multidrug combination by replacing the GW compounds with 2 polyphenols, epigallocatechin-3-gallate (E) and resveratrol (R). Sixteen rat livers were placed on NMP and assigned to control, Y defatting, Y+E+R defatting, or Y'-GW+E+R defatting groups (Y'-GW=90% dose-reduced Y defatting, n=4/group).

Results: All livers in defatting groups had significant decreases in hepatic TG content at the end of the experiment. However, livers treated with our novel Y'-GW+E+R combination had

Correspondence: William C. Chapman, Washington University School of Medicine, 660 S. Euclid Ave, Campus Box 8109, St. Louis, MO 63110. Phone: 314-362-7792; Fax: 314-361-4197; chapmanw@wustl.edu.

Authorship:

MX: Participated in research design, writing of the paper, performance of the research, and in data analysis
FZ: Participated performance of the research and in data analysis
OA: Participated in writing of the paper and performance of the research
GAU: Participated in research design and in data analysis
JJ: Participated in performance of the research
CL: Participated in performance of the research
JX: Participated in performance of the research
LY: Participated in performance of the research
SHS: Participated in performance of the research
ZZ: Participated in performance of the research
KB: Participated in data analysis
BW: Participated in research design and data analysis
J-SK: Participated in research design and data analysis
YL: Participated in research design, data analysis, and writing of the paper
WCC: Participated in research design, data analysis, and writing of the paper

Disclosure

William C. Chapman is a founder of Pathfinder Therapeutics and an advisory board of Novartis Pharmaceutical. All other authors declare no conflicts of interest.

evidence of increased metabolism, and less hepatocyte damage and carcinogenic potential. Our Y'-GW+E+R combination had increased phosphorylation of AMPK (P=0.019) and acetyl-coA carboxylase (P=0.023) compared with control; these were not increased in Y+E+R, and actually decreased in the Y groups. Furthermore, the Y'-GW+E+R group had less evidence of carcinogenic potential with no increase in AKT phosphorylation compared to control (P=0.089); the Y (P=0.031) and Y+E+R (P=0.035) groups had striking increases in AKT phosphorylation. Finally, our Y'-GW+E+R showed less evidence of hepatocyte damage with significantly lower perfusate ALT (P=0.007) and AST (P=0.014) levels.

Conclusions: We have developed a novel multidrug combination demonstrating promising defatting efficacy via activation of the AMPK pathway with an optimized safety profile and reduced hepatotoxicity during ex vivo NMP.

Supplemental Visual Abstract; http://links.lww.com/TP/C139

Introduction

The shortage of donor liver is accelerating and it has been predicted that the liver utilization could fall to 44% by 2030, resulting in over 2000 fewer liver transplants.[1] In an effort to meet liver transplant needs, organs from living donors, DCD donors, older donors (age > 70 years), and other less-than-optimal deceased donors are increasingly being considered for transplant. Presently, given the widespread epidemic of morbid obesity and diabetes in the US, hepatic steatosis is the most prevalent underlying adverse condition affecting human liver donors. Steatosis is now estimated to be present in up to 50% of deceased donor livers and is considered as the key donor variable predicting posttransplant allograft function.[2] Steatosis can affect liver allograft function and posttransplant recipient survival primarily due to an increase of susceptibility of the organs to ischemia/reperfusion injury (IRI).[3] The IRI reduces the success of orthotopic liver transplantation (OLT), and this is particularly problematic when highly marginal organs are utilized for transplant.[2] In comparison with lean allografts, these steatotic allografts are associated with higher risk of early allograft dysfunction (EAD) and primary nonfunction (PNF) rates.[4] There is no universally accepted measurement of liver steatosis, and most centers rely on estimates based on frozen section histological evaluation. Although many centers routinely use organs with mild macrosteatosis (usually defined as <20% macrosteatosis via histological estimation), the presence of moderate (30%-59% macrosteatosis) to severe steatosis (>60% macrosteatosis) has been estimated to account for up to 40% of unused and discarded liver allografts.[5,6]

The mechanisms underlying IRI in steatotic livers differ significantly from those underlying similar injuries in lean livers, but appear to be directly proportional to the degree of steatosis.[7-9] Steatotic livers have a predominance of rapid necrotic cell death, which may be related to altered energy homeostasis in these livers.[7,8,10] Endoplasmic reticulum (ER) stress is an important link between hepatic steatosis, insulin resistance, and metabolic syndrome.[11] The concept of "defatting" moderate and severely steatotic donor livers for clinical transplantation has been discussed since 2009 but has not yet been realized. While it is known that certain moderately steatotic liver grafts will provide suitable long-term function, they are associated with significantly increased complications and the risk of

PNF. Liver remodeling and resolution of macrosteatosis is known to occur in the first 7-10 days following implantation.[12] In this regard, the major risk of implanting steatotic grafts seems to relate to the heightened IRI response in the immediate time period following graft reperfusion and during the first postoperative week.

A growing interest in normothermic machine perfusion (NMP) for organ preservation is based on studies showing the efficacy and superiority of warm preservation over standard static cold storage of the liver.[13,14] NMP attenuates IRI, improves hemodynamics of the liver, recovers grafts insulted with warm ischemia, and mitigates unexpected clinical events.[15,16] In addition, NMP reduces hepatocellular damage and maintains normal bile production[17] along with improving liver transplant survival in animal models.[18] Rather than hypothermia to reduce oxygen demand, NMP provides an oxygenated perfusate to meet hepatocellular metabolic demands during organ preservation. This avoids the need for hypothermia, providing the necessary oxygen and nutrients to maintain normal cellular metabolic pathways at a physiologic temperature to address 2 important mediators of preservation injury: hypoxia and hypothermia.[19] Importantly, NMP allows an assessment phase of liver functional performance, including the ability to assess lactate clearance, maintenance of stable perfusate pH, glucose utilization, and production of adequate alkaline bile, among other parameters.[20,21]

It has been demonstrated by Nagrath et al[22] that perfusate targeting multiple pathways of hepatic lipid metabolism, such as beta-oxidation and the xenobiotic pathway, was effective in decreasing intracellular lipid content by more than 50% during 3 hours of steatotic rat liver perfusion. These components included GW7647 (peroxisome proliferator-activated receptor-alpha agonist, PPAR-alpha), GW501516 (PPAR-beta/delta agonist), pregnane X receptor ligand hypericin (HPC), the constitutive androstane receptor ligand scoparone (SCO), the glucagon mimetic and cAMP activator forskolin, and the insulin-mimetic adipokine visfatin. A study from the University of Birmingham (UK) used the same 6-drug defatting regimen to reduce tissue triglycerides by 38% and macrovesicular steatosis by 40% over 6 hours in discarded human livers during normothermic machine perfusion.[23] While these results were promising, 1 issue with this defatting combination is that the insulin mimetic action of visfatin was highly controversial, as its described biological function was not able to be replicated by other groups, resulting in the retraction of the original article.[24,25] Furthermore, several studies also indicated that administration of GW compounds was associated with hepatic carcinogenesis[26,27] as well as mitochondrial dysfunction[28,29] that consequently could lead to additional liver injury during NMP. These issues with visfatin, GW7647, and GW501516 make their use as a part of a defatting strategy untenable in the setting of human liver transplantation. To address these concerns, we propose a novel strategy to facilitate “defatting” of steatotic livers using machine perfusion in rodent models to convert otherwise discarded livers to acceptable organs for transplantation.

Materials and Methods

Animals, rat liver procurement, and NMP

Animal experiments were approved by the Washington University Animal Studies Committee. Male obese Zucker rats aging at 12-15 weeks served as liver donors (Charles River Labs, New York, NY), while lean Zucker or Lewis rats at 15 weeks of age were blood donors. Briefly, the anesthesia of animal was induced with 4% and maintained with 2% isoflurane in oxygen flow. The obese Zucker rat livers were recovered as previously described[30] and around 70mL to 110mL whole rat blood were collected from the lean rat blood donors for further use. A modified NMP system based on the Harvard Apparatus (Holliston, MA) machine perfusion was used to perform the defatting experiments (Fig 1a). Due to a suboptimal oxygenation, the primary oxygenator was replaced by a Medtronic oxygenator with a priming volume of 48ml (Affinity Pixie, BBP241). The total perfusate volume ranged from 60mL to 110mL. The perfusate samples were collected at baseline (0hr), 15m, 1hr, 2hr, 3hr, and 4hr of NMP for blood gas, basic metabolic panel, and liver enzyme tests (steatotic rat livers, n=4 for the control, and n= 5 for all other groups). The defatting multidrug combination or placebo were delivered at 1hr NMP when the system temperature and blood gas parameters were stabilized. The rat liver tissue was collected from the left lateral lobe at 0hr and 4hr for histology and further studies.

In addition, we also designed novel rat liver NMP system to examine the drug toxicity and reduce the experimental cost by replacing the Medtronic Pixie oxygenator with 2 miniature oxygenators that only have a overall prime volume less than 2ml (OX, Living system). This modification allowed us to reduce the perfusate volume to around 20mL, which the smallest perfusate volume so far in the rat liver NMP; the perfusate and liver sampling was done as described above (learn rat livers, n=3/group).

Development of a novel multidrug combination to defat steatotic Zucker rat liver via NMP

To address concerns of the conventional defatting multidrug combination, we proposed to discard Visfatin and replace the GW compounds with All-trans Retinoic acid to target the PPAR-β/δ receptors[31,32] and add the substrate Coenzyme A[33] to enhance the fat beta-oxidation (Table 1; item 7 to 12). We also add L. Carnitine to increase the fatty acid transport to mitochondria[34] as well as Lipase to catalyze lipoprotein/triglycerides into free fatty acid in the perfusate.[35] Furthermore, we also have tested the role of Epigallocatechin gallate (EGCG or E) and Resveratrol (R) in the process of defatting by NMP. EGCG and Resveratrol are natural polyphenols found in green tea and wine that having been reported to affect fat metabolism via AMPK pathway[36-39] and inflammation via NF-κB[40] and or STAT3[41] pathways. The AKT pathway is known to be associated with carcinogenesis[42] and was also investigated in our studies to confirm the potential carcinogenic risk of GW compounds. Furthermore, we attempted to lower the drug toxicity while preserving the defatting efficacy by reducing the doses of the defatting agents (Table 1; Item 4 to 8). To assess the safety and efficacy of our proposed defatting plan comparing with that used in previous studies, we performed 4 groups of Zucker rat fatty liver NMP using a whole blood-based perfusate with different defatting components as shown in Table 1: 1) Control group (n=4): supportive drugs (Heparin 100u/hr, insulin 5u/hr, Flolan 1μg/hr,

Cefazolin, 40μM, and Sodium Taurocholate) supplemented with 60ul DMSO equal to that in the defatting groups; 2) Yarmush formula defatting (Y Defatting, n=5): Table 1; item 1 to 6; 3) Yarmush formula + EGCG + Resveratrol defatting (Y+E+R Defatting, n=5); 4); Dose-reduced Yarmush formula without GW compounds + EGCG + Resveratrol defatting (Y'-GW+E+R Defatting, n=5): items 4 to 8 at the lower doses and item 9 to 12 (Table 1).

Hematoxylin and eosin staining and Immunofluorescence staining

The liver tissue was fixed by 10% formalin and paraffin-embedded or snapped frozen by liquid nitrogen, and cut with a thickness of 5μm. Hematoxylin and eosin (H&E) staining were performed using a standard protocol. The histologic assessment was performed by a liver pathologist in a blinded fashion. Immunofluorescence (IF) staining was performed to localize various relevant proteins using the following antibodies: CPT-1a (ab128568, abcam), Proliferating Cell Nuclear Antigen (PCNA, CST#2586S), and cleavage caspase-3 (CCP-3, CST# 9661). Photomicrographs were performed with Zeiss Observer Z1 immunofluorescence microscope and images were captured by Axiovision 4.8.2 software.

Western blotting and qRT-PCR

Approximately 100mg of frozen tissue was homogenized at 4°C using a homogenizer 3 times for 10-15 seconds each in 10 volumes of RIPA lysis buffer with proteases and phosphorylase inhibitors. The homogenate was centrifuged for 15 minutes at 13,000 rpm at 4°C to pellet the nuclei and particulate matter. The protein concentrations of supernatants were measured using an Invitrogen kit (Q33211, Invitrogen). For each sample, 30 to 50 μg/well of total protein lysate was loaded into a 4-12% Nu-PAGE Bis-Tris gel (Invitrogen) and subjected to electrophoresis at 80 to 120V. The protein was then transferred to a PVDF membrane (1620177, BIO-RAD) in a semidry apparatus at 30 V for 90 minutes. The membrane was blocked with 5% milk and incubated with primary antibodies, diluted 1:1000, and overnight at 4°C. These primary antibodies were used to detect relevant targets: Phospho-AMP-activated protein kinase α (p-AMPKα, CST#2535), total-AMPKα (t-AMPKα, CST#2532), Phospho-Acetyl-CoA Carboxylase (p-ACC, CST#3661), t-ACC (CST#3662), SirT1 (CST#8469), Carnitine Palmitoyltransferase 1α (CPT-1α, Abcam#128568), p-AKT (CST#4060), t-AKT (CST#4691), p-ERK1/2 (CST#9102), t-ERK1/2 (CST#9101), pp38MAPK (CST#4511), p38MAPK (CST#8690), PCNA (CST#2586), phospho-Nuclear Factor κB p65 (p-NFκBp65, CST#3033), t-NFκBp65 (CST#2535), phospho-signal transducer and activator of transcription 3 (p-STAT3, CST#9131), t-STAT3 (CST#9139), Caspase-3 (CCP-3, CST#9661), CCP-9 (CST#9508), and β-actin (CST#3700). The secondary goat anti-rabbit (CST#7074) or anti-mouse immunoglobulins (CST#7076) was diluted at 1:2000 to visualize the targets accordingly. Total mRNA was extracted using the Qiagen RNeasy Mini Kit (74104, Qiagen) according to the manufacture's instruction and mRNA concentrations were measured with Qubit assays (Q32852, Invitrogen). The cDNA was created from reverse transcription of 1.0 μg of total RNA (205311, Qiagen) to conduct qPCR analysis. Each 10μL PCR reaction mix contained: 5μL TaqMan fast master mix, 0.5μL assay mix, 1μL sample, 3.5μL H_2O. The assay mixes of *pyruvate dehydrogenase kinase, isozyme 4* (*pkd4*, Rn00585577_m1), *fatty acid binding protein 1* (*fabp1*, Rn00664587_m1), *fabp2* (Rn00565061_m1), *carnitine palmitoyltransferase 1a* (*cpt1a*, Rn00580702_m1), *bone morphogenetic protein 4* (*bmp4*,

Rn00432087_m1), notch1 (Rn01758633_m1), *jagged 2* (jag2, Rn00439932_m1), *pcna* (Rn01514538_g1), *il1a* (Rn00566700_m1), *il1b* (Rn00580432_m1), *il6* (Rn01410330_m1), *il17a* (Rn01757168_m1), *tgfb1* (Rn01418715_m1), *ccl2* (Rn00580555_m1), *Actb* (Rn00667869_m1), *Gapdh* (Rn01775763_g1) were purchased from Thermo Fisher scientific. The samples were examined in duplicate and GAPDH was used as housekeeping gene. The qPCR was performed on an ABI prism 7000 machine. In the linear range of the amplification, amplification curves were analyzed to obtain the cycle threshold (Ct) value. All gene expressions were normalized to the housekeeping gene, and fold change of expressions were calculated using delta value methods.

Data and statistical analysis

GraphPad Prism 7 software (San Diego, CA) was used to generate graphs. The results are presented as mean ± SEM. The student's *t*-test was used to compare the differences between studying groups. *P*-values less than 0.05 were considered significant.

Results

Steatotic zucker rat liver NMP and viability assessment

With our NMP parameters, there were no significant differences between the control and defatting groups in terms of portal venous pressures, perfusate flow, core liver temperature, hematocrit and potassium levels, demonstrating a consistency in our NMP technique (Fig 1b-f). Previous studies suggested that perfusate parameters such as lactate clearance, glucose utilization, and pH value are reliable makers to assess liver viability during NMP.[21] As shown in the Fig 1g and h, glucose levels dropped after a peak at the 15th minute mark, indicating glucose utilization by the livers. In addition, lactate levels cleared to around 2.2 mmol/L at 2 hours on NMP in all 4 groups, suggesting the rat livers were still viable at the end of NMP without or with defatting treatments. Despite the successful clearance of lactate, the pH level demonstrated an unexpected drop in all groups, accompanying a significant rise in the anion gap (Fig 1j); this suggests the presence of other unidentified events causing metabolic acidosis, for instance, hemolysis during NMP under our experimental conditions.

Novel defatting multidrug combination effectively reduced hepatic lipid content and liver toxicity In our study, we investigated the efficacy of Yarmush (Y) defatting (GW7647, GW501516, hypericin, scoparone, forskolin, and visfatin), Y+ epigallocatechin-3-gallate (E) + resveratrol (R) defatting, or Y' (dose-reduced Y) +E+R defatting. Histologic examination of liver biopsies showed that the hepatic architecture was well preserved after NMP in the control and defatting groups (Fig 2a). Compared to baseline (0h), both the H&E and Nile red staining indicated the lipid content decreased after 4 hours of NMP in the Y, Y+E+R, and Y'-GW+E+R defatting groups, while there was no apparent change in the control group (Fig 2a, b). There was no significant change of the liver weight between before and after NMP among the control and defatting groups (Fig 2c). As shown in Fig 2d&e, there was no significant difference in liver TG content at baseline. When compared to the control group at 4 hours of NMP, all defatting groups had a significant decrease in hepatic TG concentrations (Control vs Y defatting, P=0.016; control vs Y+E+R defatting, P=0.006; control vs Y'-GW+E+R defatting, P=0.013). To address any potential variations

from the different experimental parameters, the perfusate ALT (Fig 2f) and AST (Fig 2g) concentrations were adjusted by perfusate volume and liver weight at 15 minutes on NMP and afterward. the Y'-GW+E+R defatting group had significantly lower perfusate ALT (Control vs Y'-GW+E+R defatting, P=0.007; Y defatting vs Y'-GW+E+R defatting, P=0.026, Y+E+R defatting vs Y'-GW+E+R defatting, P=0.319). The AST levels were also found with a similar changing trends (Control vs Y'-GW+E+R defatting, P=0.014; Y defatting vs Y'-GW+E+R defatting, P=0.013; Y+E+R defatting vs Y'-GW+E+R defatting, P=0.057). In summary, our modified defatting agents had the defatting efficacy compared with the conventional defatting plan but with significantly less hepatotoxicity.

To further test the toxicity of our new defatting drug combination, we also compared the outcomes of the rat liver NMP with or without Y'-GW+E+R defatting using lean rat livers and our modified system with a total perfusate volume around 20mL. The Fig 3 shows the circuit settings and the perfused livers at 15min, 1hr, 2hr, 3hr, and 4hr NMP with an optimal oxygenation (pO2 around 70-300mmHg) and ventilation (pCO2 around 30-60mmHg). Perfusate volume, donor body weight and liver weight, bile production, bile bicarbonate, bile glucose and bile lactate were similar between 2 groups (Fig 3b-3h). The portal pressure and flow as well the perfusate parameters (Fig 3i-3u) including lactate clearances and histology (Fig 3v) were comparable between the control and defatting groups. These data suggest that the Y'-GW+E+R defatting combination did not induce hepatotoxicity in our study. Furthermore, we performed a NMP experiment without liver in the circulation and found a similar changing pattern of perfusate pH value and anion gap compared to that in the NMP with lean rat livers (Fig S1 http://links.lww.com/TP/C129).

Our novel defatting multidrug combination removed liver fat content via activation of AMPK pathway Activation of the AMPK pathway has been reported to increase cellular energy utilization and fat metabolism.[36-39] To explore the mechanisms of our new defatting strategy, we investigated the AMPK pathway before and after NMP with or without defatting treatment (Fig 4a, b). The changes of biomarker expression at the end of NMP were standardized by its expression at baseline for further analysis. When compared to the control group, AMPK phosphorylation, an event indicative of AMPK activation, was significantly increased in the Y'-GW+E+R defatting group (P=0.019) while significantly decreased in the Y defatting (P=0.026) but not the Y+E+R defatting group (P=0.084), suggesting the presence of distinct defatting mechanisms between Y and Y'-GW+E+R. However, we did not observe significantly increased defatting capacity in the Y+E+R than other defatting groups, suggesting that targeting these 2 pathways at the same time was not additive with regards to the defatting efficacy (Fig 2d). In parallel to the increase of AMPK phosphorylation, we also found that the phosphorylation level of acetyl-CoA carboxylase (ACC) (Fig 4c) was significantly higher in the Y'-GW+E+R defatting group than that in the control group (P=0.023). Carnitine palmitoyltransferase-1α (CPT-1A) expression showed a similar change (Fig 4e, Control vs Y'-GW+E+R, P=0.024). By RT-PCR as shown in Fig 4f, i, the gene expression of pyruvate dehydrogenase kinase, isozyme 4 (*pkd4*) was significantly increased in the Y'-GW+E+R defatting group than in the control group (P=0.043). *Cpt-1a* expression was also significantly higher in the Y+E+R defatting group than that in the Y defatting (P=0.016) and Y'-GW+E+R defatting groups (P=0.009). No significant changes were found with regard of *fabp1* and *fabp2* gene expression among all groups (Fig 4g, h).

The current defatting multidrug combination decreased the risk of hepatocyte proliferation during NMP It has been shown that the activation of the AKT pathway significantly increases cell proliferation and the risk of carcinogenesis.[42,43] In our study, we also found that there were striking increases of AKT phosphorylation in the Y and Y+E+R defatting groups compared to the control group (P=0.031 and 0.035, respectively), while there was no significant change of the AKT phosphorylation in the Y'-GW+E+R defatting group compared to the control group (P=0.089; Fig 5a, b). To evaluate the effects of GW compounds on cell proliferation, we studied several related biomarkers. The changes of ERK phosphorylation were present in a similar fashion (Fig 5a, c): Control vs Y defatting, P=0.040; Control vs Y+E+R defatting, P=0.223; Control vs Y'-GW+E+R defatting, P=0.138. Furthermore, the protein expression of proliferating cell nuclear antigen (PCNA) was significantly upregulated in the Y defatting and Y+E+R defatting group than that in the control group (P=0.049 and 0.004, respectively), but not in the Y'-GW+E+R defatting group (Fig 5e, j). Our data from qRT-PCR also showed an increase of the hepatic *pcna* mRNA level with 3 hours NMP defatting with GWs (Fig 5i). The *bone morphogenetic protein*-4 (*Bmp-4*) expression was significantly increased in the Y'-GW+E+R defatting group than that in the control group (Fig 5f, P=0.008). The *Jagged 2* (*Jag2*) mRNA levels were lower in the Y defatting and Y+E+R defatting group than that in the control group (Fig 5h, P=0.127 and 0.083, respectively). However, *pcna* gene expression was marginally higher in the Y defatting and Y+E+R defatting group than that in the control group (Fig 5i, P=0.057 and 0.067, respectively). No significant changes were found with regard of *notch1* gene expression among all groups (Fig 5g). Taken together, the treating with GW compounds increased cell proliferation in the setting of rat liver NMP.

Our novel defatting multidrug combination reduced the hepatic apoptosis during NMP

Of note, we used whole blood for NMP, allowing for the evaluation the effects of each defatting regimen on several cytokine-signaling pathways as well as cytokines such as IL-1, IL-6, IL-17, TGF-b, and CCL-2 etc. Our study demonstrated a significant decrease in phosphorylated nuclear factor kappa-light-chain-enhancer of activated B cells (NF-κBp65) in the Y and Y+E+R defatting groups compared to control, while no significant change was found in the Y'-GW+E+R defatting group (P=0.557, Fig 6a,b). In contrast, the phosphorylation of STAT3 in the Y and Y+E+R defatting groups were significantly decreased compared to control (P=0.039 and 0.045, respectively), while no significant change was found in the Y'-GW+E+R defatting group (P=0.237, Fig 6c). Importantly, we found that the expression of cleaved caspase 9 (CCP9) was significantly higher in the Y defatting than that in the control group (P=0.041, Fig 6d). Moreover, the cleaved caspase 3 (CCP3) in Y defatting and Y+E+R defatting were significantly increased than that in the control group (P=0.014 and 0.022, respectively), while it was significantly decreased in the Y'-GW+E+R defatting group (P=0.010, Fig 6e). As shown in Fig 6f-k, the cytokine gene expression was largely depressed in the Y defatting and Y+E+R defatting group than that in the control group but unchanged in the Y'-GW+E+R defatting group. In summary, the treatments containing GW compounds decreased the NF-κB signaling and increased the hepatic apoptosis. Our novel multidrug combination achieved promising defatting efficacy via activation AMPK pathway and the hepatotoxicity was significantly reduced (Fig 7).

Discussion

Given that livers with high levels of macrosteatosis are more prone to IRI, our goal is to evaluate the potential effects of reconditioning livers using defatting agents to reduce the level of steatosis and thus IRI after transplantation. Adenosine monophosphate-activated protein kinase (AMPK) is an intracellular energy sensor seen to play a central role in regulation of glucose and lipid metabolism with studies suggesting its activation in cellular energy depletion.[44] Subsequent activation leads to the upregulation of catabolic pathways, most importantly fatty-acid and glucose oxidation, while reducing ATP consuming anabolic pathways such as triglyceride and cholesterol synthesis.[45] Epigallocatechin-3-gallate (EGCG) is a polyphenol commonly found in green tea with several studies regularly emphasizing its anti-oxidant potential.[46] EGCG appears to enhance AMPK phosphorylation and contribute further to energy dependent metabolic activities.[47] In a murine model, the treatment of cells with EGCG resulted in a dose dependent increase in AMPKα and subsequent AMPK activation.[48] Additional studies have attempted to define the specific mechanism of AMPK activation by EGCG with evidence suggesting that this is mediated through a Ca^{2+}/calmodulin-dependent protein kinase (CaMKK). It has also been proposed that EGCG activates the AMPK pathway by manipulating the ratios of AMP/ADP/ATP.[49] Another possibility is EGCG dependent inhibition of mitochondrial oxidative phosphorylation decreasing ATP levels leading to the subsequent activation of AMPK in response to the falling energy status within a cell.[50] Drawing some similarities to EGCG, resveratrol – induced activation of AMPK is facilitated through several mechanisms with evidence suggesting variations among cell types.[51] Resveratrol was initially described as a SIRT-1 activator of AMP-activated protein kinase (AMPK), but later studies suggested further complexity in its role within this pathway.[52] Resveratrol appears to activate AMPK through an energy dependent ATP synthase inhibition pathway and energy independent SIRT1-LKB1 activation. In our study, there was a significant increase in AMPK phosphorylation in livers defatted with Y'-GW+EGCG+Resveratrol, which is also supported in other studies whereby Resveratrol appeared to induce AMPK activation through a phosphorylation process in hepatic tissues. This supports its impact on metabolic tissue and particularly its lipid lowering ability[53] and also leads to the downstream expression of carnitine palmitoyl transferase-I (CPT-I) and medium-chain acyl-COA dehydrogenases further facilitating cellular fatty acid oxidation.[54] On the other hand, the peroxisome proliferator-activated receptors (PPARs) are transcription factors regulating diverse physiological and pathological processes including cell growth, morphogenesis, differentiation, and homeostasis.[55] PPAR-α (GW7647) and δ (GW501516) agonists have been largely reported to activate AMPK signaling in a receptor-independent manner.[56] Specifically, GW7647 has been shown to induce AMPK phosphorylation and its downstream protein target acetyl-CoA carboxylase;[57] GW501516 similarly activates the AMPK pathway.[58] Surprisingly, we didn't observe a significant increase of AMPK phosphorylation in the defatting groups with GW compounds (Y defatting and Y+E+R defatting group) in our current study. The AMPK phosphorylation in the Y defatting group was even lower than that in the control group. The mechanism of this unexpected result is difficult to know due to the complexity of these multidrug defatting multidrug combination. However, we do notice that 1 of the defatting components, forskolin, has been shown to be

able to inhibit AMPK activity and reduce phosphorylation of the activation loop α-Thr172 via inhibition of calcium/calmodulin-dependent protein kinase kinase-α and β,[59] which may reduce or reverse the overall effect AMPK activation induced by GW compounds or EGCG and Resveratrol. However, in the Y'-GW+E+R defatting group, AMPK activation was well-preserved due to the decreased effects of forskolin at a lower dose. Consequently, the lipid metabolism mediated by AMPK was maintained at a lower hepatotoxicity suggested by the favorable ALT/AST levels and Caspase-3 expression in this defatting group.

There were significant increases of AKT and ERK1/2 phosphorylation in the defatting groups with PPAR-α (GW7647) and δ (GW501516) agonists in our current study. Furthermore, results of qRT-PCR and immunoblotting showed a significant increase in hepatic PCNA protein expression at the end of NMP in defatting groups using GW compounds, suggesting a significant increase of hepatocyte proliferation similar to the results of previous studies in hepatocyte proliferation under special circumstances.[60,61] These findings justify the removal of the GW compounds from the defatting multidrug combination to eliminate the associated risks of carcinogenesis. Previous studies have demonstrated the feasibility of NMP as a tool to promote liver regeneration and reduce the inflammatory response over a short period of perfusion before human liver transplantation.[20,21] In the setting of our experiment, the use of whole blood-based perfusate allowed for the evaluation of inflammatory responses amid the different defatting treatments. In the defatting groups with GW compounds, the NFkB pathway was significantly depressed; consequently, most cytokine gene transcription was decreased but accompanied by rising CCP-3 and ALT/AST levels, suggesting that the defatting multidrug combination in these 2 groups could affect the hepatocytes and hepatic inflammatory cells simultaneously.

One of the obvious limitations in our study is that the liver grafts were not implanted in the recipient rats. Therefore, it is hard to know the real benefits of the defatting treatments. Although the perfusate lactate and liver enzymes supported that the liver grafts were viable after defatting treatment, the PH value was dropping and the anion gap was increasing, which could be associated with the mechanical damage from the roller pump to the red blood cell indicated by the gradual red discoloration of the perfusate plasma, decreasing hematocrit, and rising potassium and phosphate levels. Further improvement of the rat NMP system or using pig model with clinically proved device such as OrganOx Metra would solve the mechanical issue and make long-term survival possible after NMP liver transplant.

In conclusion, we developed a novel multidrug combination that achieved promising defatting efficacy via activation AMPK pathway while the hepatotoxicity was significantly reduced during ex vivo NMP.

Supplementary Material

Refer to Web version on PubMed Central for supplementary material.

Acknowledgments

This project was supported in part by the Barnes-Jewish Hospital Foundation Project Award, Transplant Research. Thanks to the Digestive Diseases Research Core Centers (DDRCC, NIDDK P30 DK052574) at WUSM for sharing equipment and core facility support.

Funding:

This project was funded in part by the Barnes-Jewish Hospital Foundation Grant 4776 (J-SK) and 7556 (WCC), Transplant Research, National Institutes of Health grant R01DK07987911 (J-SK). Thanks to the Digestive Diseases Research Core Centers (DDRCC, NIDDK P30 DK052574) at WUSM for sharing equipment and core facility support.

Abbreviations:

IRI	Ischemia-Reperfusion Injury
NMP	Normothermic Machine Perfusion

References

1. Orman ES, Mayorga ME, Wheeler SB, et al. Declining liver graft quality threatens the future of liver transplantation in the United States. Liver Transplant. 2015;21(8):1040–1050.
2. Nocito A, El-Badry AM, Clavien P-A. When is steatosis too much for transplantation? J Hepatol. 2006;45(4):494–499. [PubMed: 16919359]
3. Durand F, Renz JF, Alkofer B, et al. Report of the Paris consensus meeting on expanded criteria donors in liver transplantation. Liver Transplant. 2008;14(12):1694–1707.
4. McCormack L, Petrowsky H, Jochum W, et al. Use of severely steatotic grafts in liver transplantation: a matched case-control study. Ann Surg. 2007;246(6):940–946. [PubMed: 18043095]
5. Escartin A, Castro E, Dopazo C, et al. Analysis of discarded livers for transplantation. Transplant Proc. 2005;37(9):3859–3860. [PubMed: 16386563]
6. Sayuk GS, Leet TL, Schnitzler MA, Hayashi PH. Nontransplantation of livers from deceased donors who are able to donate another solid organ: how often and why it happens. Am J Transplant. 2007;7(1):151–160. [PubMed: 17227564]
7. Chavin KD, Fiorini RN, Shafizadeh S, et al. Fatty acid synthase blockade protects steatotic livers from warm ischemia reperfusion injury and transplantation. Am J Transplant. 2004;4(9):1440–1447. [PubMed: 15307831]
8. Evans ZP, Ellett JD, Schmidt MG, et al. Mitochondrial uncoupling protein-2 mediates steatotic liver injury following ischemia/reperfusion. J Biol Chem. 2008;283(13):8573–8579. [PubMed: 18086675]
9. Selzner M, Rudiger HA, Sindram D, et al. Mechanisms of ischemic injury are different in the steatotic and normal rat liver. Hepatology. 2000;32(6):1280–1288. [PubMed: 11093735]
10. Marcon F, Schlegel A, Bartlett DC, et al. Utilization of Declined Liver Grafts Yields Comparable Transplant Outcomes and Previous Decline Should Not Be a Deterrent to Graft Use. Transplantation. 2018;102(5):e211–e218. [PubMed: 29702538]
11. Anderson CD, Upadhya G, Conzen KD, et al. Endoplasmic reticulum stress is a mediator of posttransplant injury in severely steatotic liver allografts. Liver Transpl. 2011;17(2):189–200. [PubMed: 21280192]
12. Posner AD, Sultan ST, Zaghloul NA, et al. Resolution of donor non-alcoholic fatty liver disease following liver transplantation. Clin Transplant. 2017;31(9).
13. Schlegel A, Kron P, Graf R, et al. Warm vs. cold perfusion techniques to rescue rodent liver grafts. J Hepatol. 2014;61(6):1267–1275. [PubMed: 25086285]

14. Cardini B, Oberhuber R, Fodor M, et al. Clinical Implementation of Prolonged Liver Preservation and Monitoring Through Normothermic Machine Perfusion in Liver Transplantation. Transplantation. 2020;104(9):1917–1928. [PubMed: 32371845]
15. Izamis ML, Tolboom H, Uygun B, et al. Resuscitation of ischemic donor livers with normothermic machine perfusion: a metabolic flux analysis of treatment in rats. PloS ONE. 2013;8(7):e69758. [PubMed: 23922793]
16. Carvalheiro AP, McKay SC, Bartlett DC, et al. Novel Use of Normothermic Machine Perfusion of the Liver: A Strategy to Mitigate Unexpected Clinical Events. Transplantation 2020;104(9):e281–e282. [PubMed: 32826844]
17. op den Dries S, Karimian N, Sutton ME, et al. Ex vivo normothermic machine perfusion and viability testing of discarded human donor livers. Am J Transplant. 2013;13(5):1327–1335. [PubMed: 23463950]
18. Brockmann J, Reddy S, Coussios C, et al. Normothermic perfusion: a new paradigm for organ preservation. Ann Surg. 2009;250(1):1–6. [PubMed: 19561463]
19. Fondevila C, Hessheimer AJ, Maathuis MH, et al. Superior preservation of DCD livers with continuous normothermic perfusion. Ann Surg. 2011;254(6):1000–1007. [PubMed: 21862925]
20. Jassem W, Xystrakis E, Ghnewa YG, et al. Normothermic Machine Perfusion (NMP) Inhibits Proinflammatory Responses in the Liver and Promotes Regeneration. Hepatology. 2019;70(2):682–695. [PubMed: 30561835]
21. Nasralla D, Coussios CC, Mergental H, et al. A randomized trial of normothermic preservation in liver transplantation. Nature. 2018;557(7703):50–56. [PubMed: 29670285]
22. Nagrath D, Xu H, Tanimura Y, et al. Metabolic preconditioning of donor organs: defatting fatty livers by normothermic perfusion ex vivo. Metab Eng. 2009;11(4-5):274–283. [PubMed: 19508897]
23. Boteon YL, Attard J, Boteon A, et al. Manipulation of Lipid Metabolism During Normothermic Machine Perfusion: Effect of Defatting Therapies on Donor Liver Functional Recovery. Liver Transpl. 2019;25(7):1007–1022. [PubMed: 30821045]
24. Fukuhara A, Matsuda M, Nishizawa M, et al. Visfatin: a protein secreted by visceral fat that mimics the effects of insulin. Science. 2005;307(5708):426–430. [PubMed: 15604363]
25. Fukuhara A, Matsuda M, Nishizawa M, et al. Retraction. Science. 2007;318(5850):565.
26. Klaunig JE, Babich MA, Baetcke KP, et al. PPARalpha agonist-induced rodent tumors: modes of action and human relevance. Crit Rev Toxicol. 2003;33(6):655–780. [PubMed: 14727734]
27. Peters JM, Cheung C, Gonzalez FJ. Peroxisome proliferator-activated receptor-alpha and liver cancer: where do we stand? J Mol Med. 2005;83(10):774–785. [PubMed: 15976920]
28. Brunmair B, Lest A, Staniek K, et al. Fenofibrate impairs rat mitochondrial function by inhibition of respiratory complex I. J Pharmacol Exp Ther. 2004;311(1):109–114. [PubMed: 15166256]
29. Martinez B, Perez-Castillo A, Santos A. The mitochondrial respiratory complex I is a target for 15-deoxy-delta12,14-prostaglandin J2 action. J Lipid Res. 2005;46(4):736–743. [PubMed: 15654126]
30. Kamada N, Calne RY. Orthotopic liver transplantation in the rat. Technique using cuff for portal vein anastomosis and biliary drainage. Transplantation. 1979;28(1):47–50. [PubMed: 377595]
31. Rieck M, Meissner W, Ries S, et al. Ligand-mediated regulation of peroxisome proliferator-activated receptor (PPAR) beta/delta: a comparative analysis of PPAR-selective agonists and all-trans retinoic acid. Mol Pharmacol. 2008;74(5):1269–1277. [PubMed: 18701617]
32. Shaw N, Elholm M, Noy N. Retinoic acid is a high affinity selective ligand for the peroxisome proliferator-activated receptor beta/delta. J Biol Chem. 2003;278(43):41589–41592. [PubMed: 12963727]
33. Adeva-Andany MM, Carneiro-Freire N, Seco-Filgueira M, et al. Mitochondrial beta-oxidation of saturated fatty acids in humans. Mitochondrion. 2019;46:73–90. [PubMed: 29551309]
34. Banan B, Watson R, Xu M, et al. Development of a normothermic extracorporeal liver perfusion system toward improving viability and function of human extended criteria donor livers. Liver Transpl. 2016;22(7):979–993. [PubMed: 27027254]
35. Svendsen A Lipase protein engineering. Biochim Biophys Acta. 2000;1543(2):223–238. [PubMed: 11150608]

36. Chen N, Bezzina R, Hinch E, et al. Green tea, black tea, and epigallocatechin modify body composition, improve glucose tolerance, and differentially alter metabolic gene expression in rats fed a high-fat diet. Nutr Res. 2009;29(11):784–793. [PubMed: 19932867]
37. Collins QF, Liu HY, Pi J, et al. Epigallocatechin-3-gallate (EGCG), a green tea polyphenol, suppresses hepatic gluconeogenesis through 5'-AMP-activated protein kinase. J Biol Chem. 2007;282(41):30143–30149. [PubMed: 17724029]
38. Lee MS, Kim CT, Kim Y. Green tea (−)-epigallocatechin-3-gallate reduces body weight with regulation of multiple genes expression in adipose tissue of diet-induced obese mice. Ann Nutr Metab. 2009;54(2):151–157. [PubMed: 19390166]
39. Moon H-S, Chung C-S, Lee H-G, et al. Inhibitory effect of (−)-epigallocatechin-3-gallate on lipid accumulation of 3T3-L1 cells. Obesity. 2007;15(11):2571–2582. [PubMed: 18070748]
40. Chen A, Zhang L. The antioxidant (−)-epigallocatechin-3-gallate inhibits rat hepatic stellate cell proliferation in vitro by blocking the tyrosine phosphorylation and reducing the gene expression of platelet-derived growth factor-beta receptor. J Biol Chem. 2003;278(26):23381–23389. [PubMed: 12695518]
41. Lee IT, Lin CC, Lee CY, et al. Protective effects of (−)-epigallocatechin-3-gallate against TNF-alpha-induced lung inflammation via ROS-dependent ICAM-1 inhibition. J Nutr Biochem. 2013;24(1):124–36. [PubMed: 22819551]
42. Fruman DA, Chiu H, Hopkins BD, et al. The PI3K Pathway in Human Disease. Cell. 2017;170(4):605–635. [PubMed: 28802037]
43. Riggio M, Polo ML, Blaustein M, et al. PI3K/AKT pathway regulates phosphorylation of steroid receptors, hormone independence and tumor differentiation in breast cancer. Carcinogenesis. 2012;33(4):509–518. [PubMed: 22180571]
44. Park CE, Kim M-J, Lee JH, et al. Resveratrol stimulates glucose transport in C2C12 myotubes by activating AMP-activated protein kinase. Exp Mol Med. 2007;39(2):222. [PubMed: 17464184]
45. Zong H, Ren JM, Young LH, et al. AMP kinase is required for mitochondrial biogenesis in skeletal muscle in response to chronic energy deprivation. Proc Natl Acad Sci USA. 2002;99(25):15983–15987. [PubMed: 12444247]
46. Pournourmohammadi S, Grimaldi M, Stridh MH, et al. Epigallocatechin-3-gallate (EGCG) activates AMPK through the inhibition of glutamate dehydrogenase in muscle and pancreatic ß-cells: A potential beneficial effect in the pre-diabetic state? Int J Biochem Cell Biol. 2017;88:220–225. [PubMed: 28137482]
47. Wu J, Xu X, Li Y, et al. Quercetin, luteolin and epigallocatechin gallate alleviate TXNIP and NLRP3-mediated inflammation and apoptosis with regulation of AMPK in endothelial cells. Eur J Pharmacol. 2014;745:59–68. [PubMed: 25446924]
48. Murase T, Misawa K, Haramizu S, et al. Catechin-induced activation of the LKB1/AMP-activated protein kinase pathway. Biochem Pharmacol. 2009;78(1):78–84. [PubMed: 19447226]
49. Long YC, Zierath JR. AMP-activated protein kinase signaling in metabolic regulation. J Clin Invest. 2006;116(7):1776–1783. [PubMed: 16823475]
50. Valenti D, de Bari L, Manente GA, et al. Negative modulation of mitochondrial oxidative phosphorylation by epigallocatechin-3 gallate leads to growth arrest and apoptosis in human malignant pleural mesothelioma cells. Biochim Biophys Acta. 2013;1832(12):2085–2096. [PubMed: 23911347]
51. Lan F, Cacicedo JM, Ruderman N, et al. SIRT1 modulation of the acetylation status, cytosolic localization, and activity of LKB1 possible role in AMP-activated protein kinase activation. J Biol Chem. 2008;283(41):27628–27635. [PubMed: 18687677]
52. Lan F, Weikel KA, Cacicedo JM, et al. Resveratrol-Induced AMP-Activated Protein Kinase Activation Is Cell-Type Dependent: Lessons from Basic Research for Clinical Application. Nutrients. 2017;9(7):751.
53. Baur JA, Pearson KJ, Price NL, et al. Resveratrol improves health and survival of mice on a high-calorie diet. Nature. 2006;444(7117):337–342. [PubMed: 17086191]
54. Meng R-S, Pei Z-h, Yin R, et al. Adenosine monophosphate-activated protein kinase inhibits cardiac hypertrophy through reactivating peroxisome proliferator-activated receptor-α signaling pathway. Eur J Pharmacol. 2009;620(1-3):63–70. [PubMed: 19699196]

55. Ahmed W, Ziouzenkova O, Brown J, et al. PPARs and their metabolic modulation: new mechanisms for transcriptional regulation? J Intern Med. 2007;262(2): 184–198. [PubMed: 17645586]

56. Lee WH, Kim SG. AMPK-Dependent Metabolic Regulation by PPAR Agonists. PPAR Res. 2010;2010:549101. [PubMed: 20814441]

57. Xiao X, Su G, Brown SN, et al. Peroxisome proliferator-activated receptors gamma and alpha agonists stimulate cardiac glucose uptake via activation of AMP-activated protein kinase. J Nutr Biochem. 2010;21(7):621–626. [PubMed: 19570670]

58. Kramer DK, Al-Khalili L, Guigas B, et al. Role of AMP kinase and PPARdelta in the regulation of lipid and glucose metabolism in human skeletal muscle. J Biol Chem. 2007;282(27): 19313–19320. [PubMed: 17500064]

59. Hurley RL, Barre LK, Wood SD, et al. Regulation of AMP-activated protein kinase by multisite phosphorylation in response to agents that elevate cellular cAMP. J Biol Chem. 2006;281(48):36662–36672. [PubMed: 17023420]

60. Shah YM, Morimura K, Yang Q, et al. Peroxisome proliferator-activated receptor alpha regulates a microRNA-mediated signaling cascade responsible for hepatocellular proliferation. Mol Cell Biol. 2007;27(12):4238–4247. [PubMed: 17438130]

61. Xu M, Alwahsh SM, Ramadori G, et al. Upregulation of hepatic melanocortin 4 receptor during rat liver regeneration. J Surg Res. 2016;203(1):222–230. [PubMed: 24433867]

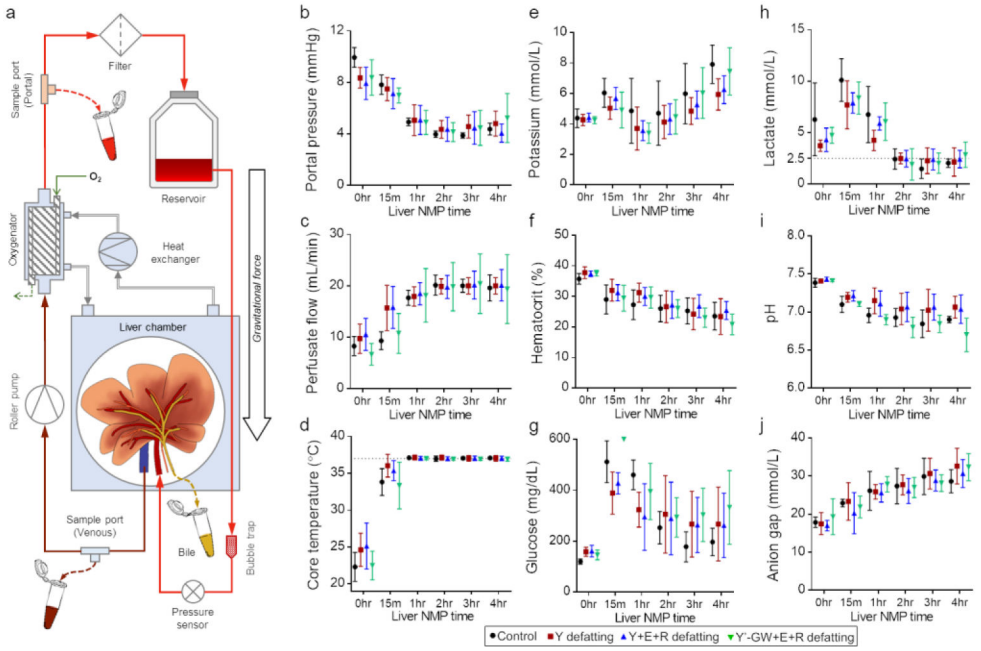

Figure 1. The normothermic machine perfusion (NMP) of rat liver.

Schematic of the NMP system used in the current study (a), the portal pressure (b), perfusate flow (c), and hepatic core temperature (d) during NMP. Perfusate levels of potassium (e), hematocrit (f), glucose (g), lactate (h), pH (i), and anion gap (j) before and during NMP of the Zucker rat livers.

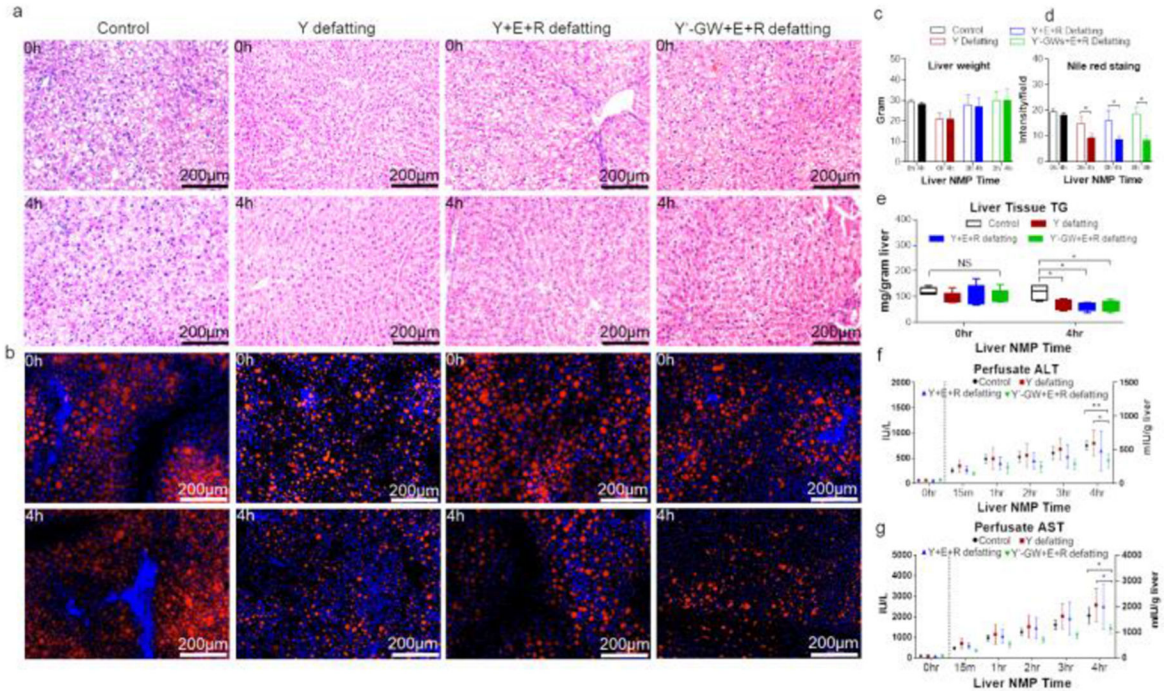

Figure 2. Defatting efficacy and drug toxicity of the defatting multidrug combination.

H&E (a) and NILE red (b) staining of rat livers; liver weight before and after NMP defatting (c); liver tissue TG before and after defatting treatments (d&e); ALT (f) and AST (g) before and during NMP.

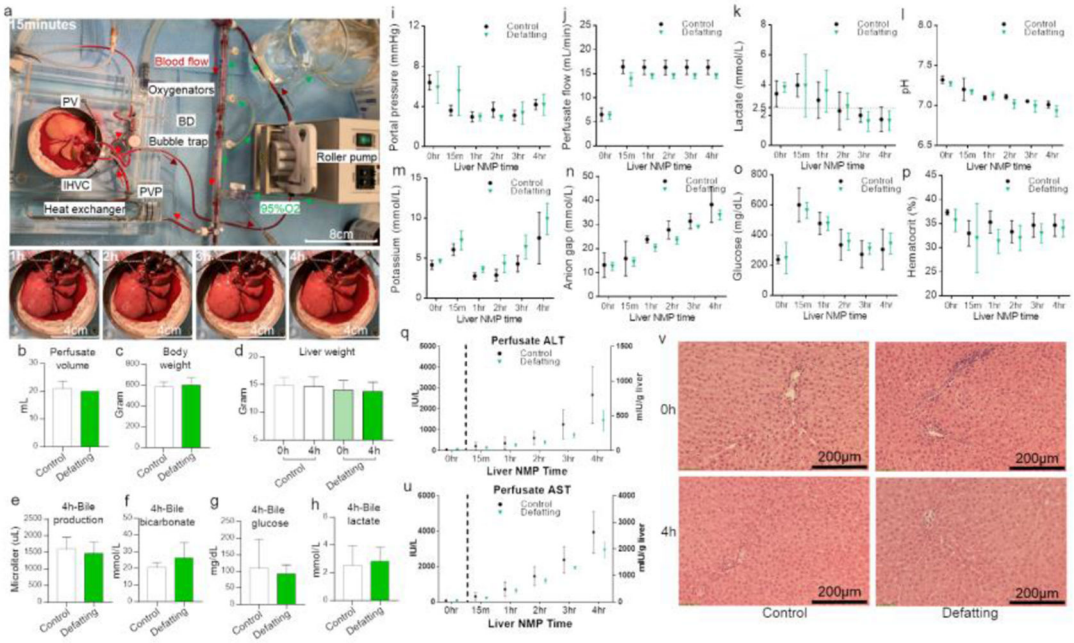

Figure 3. A novel rat liver NMP model to examine the hepatotoxicity of Y'-GW+E+R defatting.

(a) shows the circuit settings and a lean rat liver at NMP 15minutes, 1h, 2h, 3h and 4h; (b) perfusate volumes; (c) the body weight of liver donors; (d) liver weight before and after NMP defatting; (e) bile production volume: (f) bicarbonate of the bile; (g) bile glucose levels; (h) bile lactate levels. (i and j) the portal pressure an portal flow; (k-p) perfusate metabolic parameters; (q-u) perfusate ALT and AST levels; (v) H&E images of the livers before and after NMP defatting.

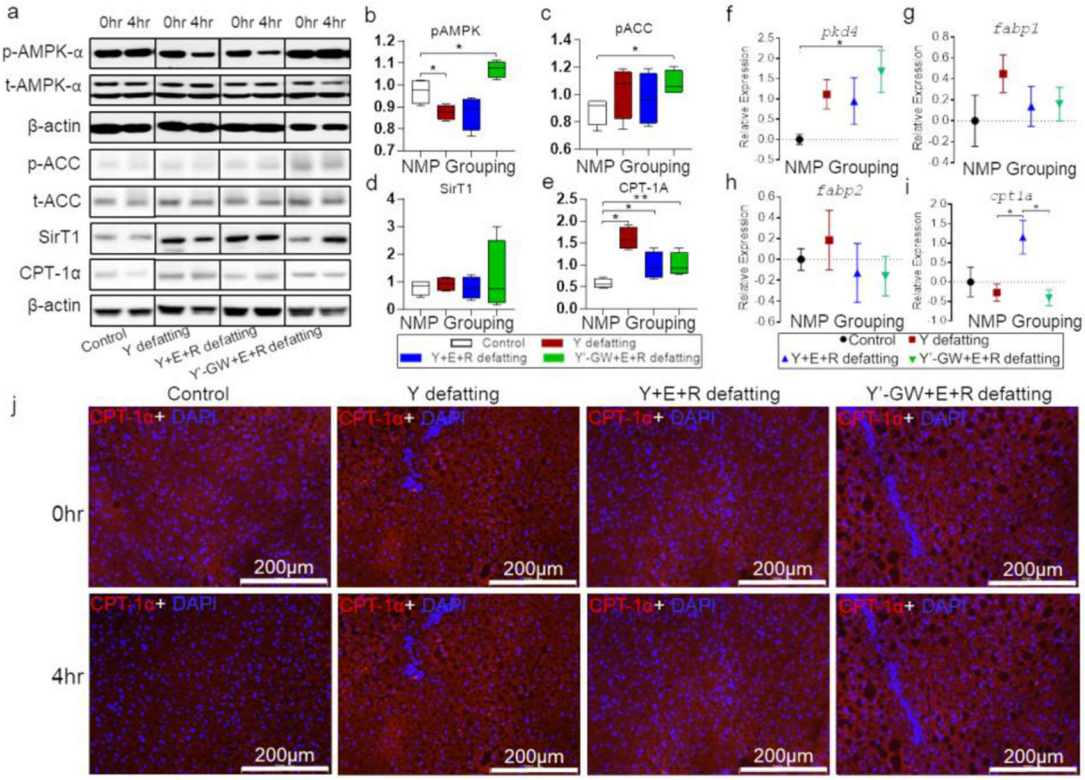

Figure 4. Fat metabolism pathways in the rat livers with different defatting multidrug combination.

(a) shows the representative immunoblotting bands of each group; the phosphorylation of AMPK (b) and ACC (c), the SirT1 (d) and CPT-1A (e) levels in the rat livers; the mRNA transcription of *pkd4* (f), *fabp1* (g), *fabp2* (h), and *cpt1a* (i) in the rat livers; j, the immunofluorescence staining of CPT-1a in the rat livers.

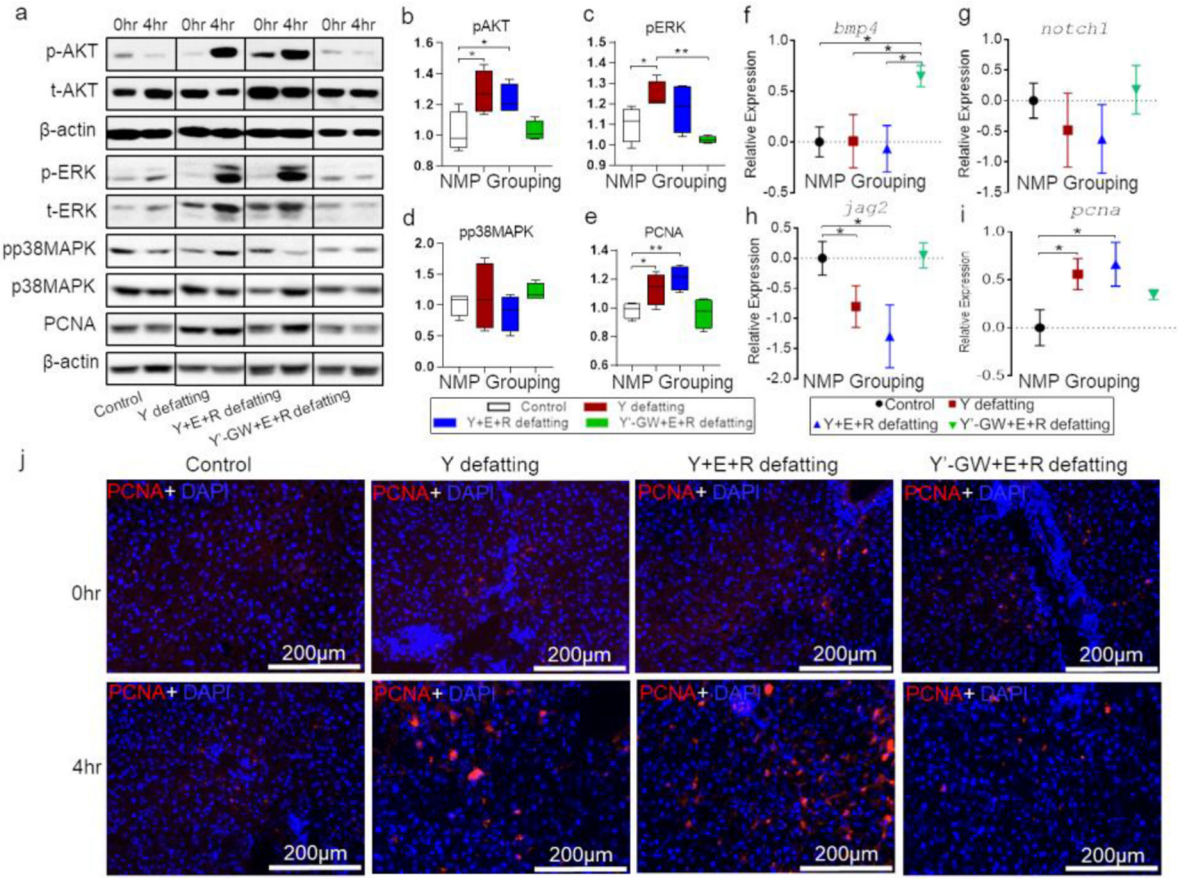

Figure 5. Cell growth and proliferation of gene expression in the rat livers with different defatting multidrug combination.

a, shows the representative immunoblotting bands of each group; the phosphorylation of AKT (b), ERK1/2 (c), p38MAPK (d), and PCNA levels (e) in rat livers; the mRNA transcription levels of *bmp4* (f), *notch1* (g), *jag2* (h), and *pcna* (i) in rat livers; (j) the immunofluorescence staining of PCNA in rat livers.

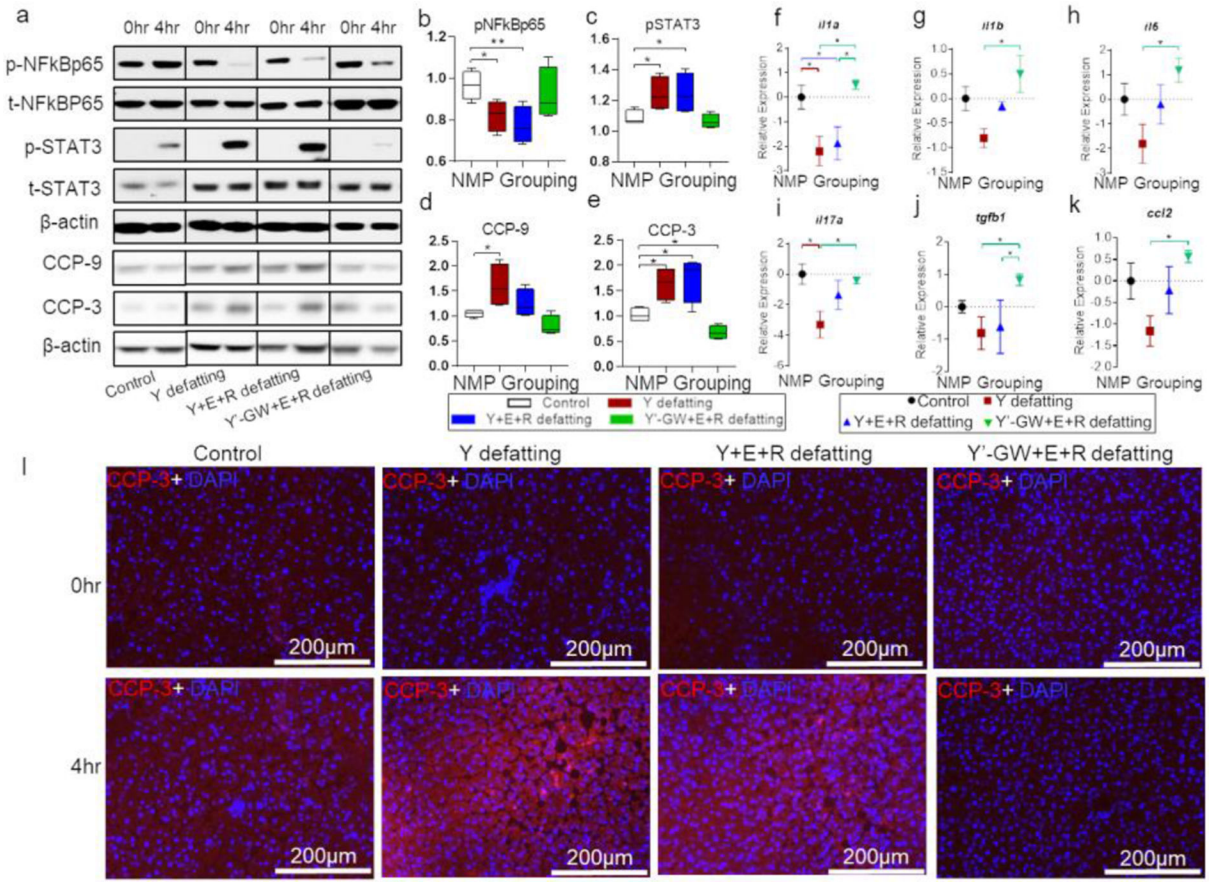

Figure 6. Inflammatory pathways and cytokine gene expression in the rat livers with different defatting multidrug combination.

a, shows the representative immunoblotting bands of each group; the phosphorylation of p-NFkBp65 (b) and p-STAT3 (c), CCP-9 (d) and CCP-3 (e) levels in the rat livers; the mRNA transcription of IL-*1a* (f), IL-*1b* (g), IL*6* (h), IL*17a* (i), TGF-*b* (j), and *ccl2* (k) in the rat livers; (l), the immunofluorescence staining of CCP-3 in the rat livers.

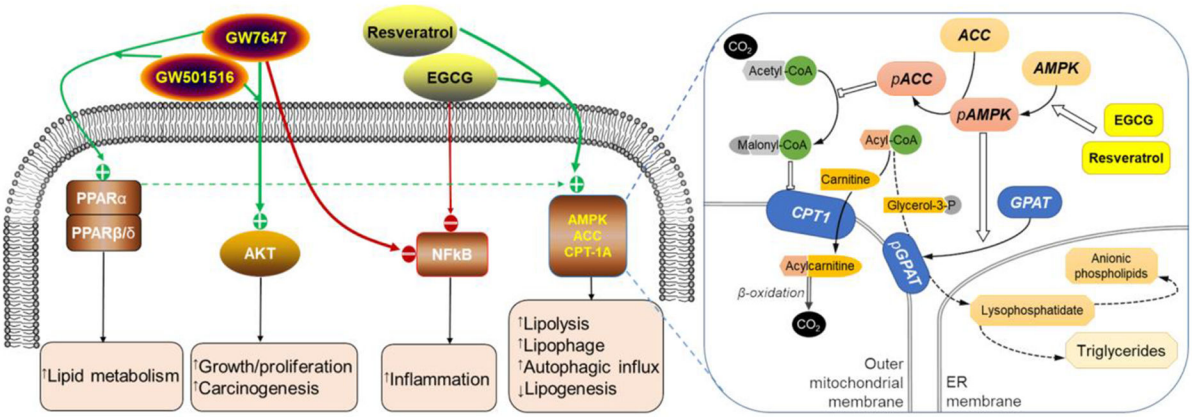

Figure 7. Schematic summary of the partial molecular pathways involved in this study.

a, the overview of relevant pathways and b, the role of AMPK pathway in fat metabolism based on the current and previous studies.

Table 1.

The formulation of defatting multidrug combination.

Code	Drug name	Dose	Function	Mechanism of action
1	*Visfatin*	*NA*	Defatting drugs used in Yarmush et al's studies	*Insulin mimetic*
2	*GW7647*	*1μM*		*PPAR-α agonist to promote* ***β-oxidation***
3	*GW501516*	*1μM*		*PPAR-β/δ agonist*
4	Forskolin	10μM or 1μM		Glucagon mimetic and cAMP activator that increases **β-oxidation** and **Ketogenesis**
5	Hypericin	10μM or 1μM		Activates pregnane X receptor (PXR), activates **xenobiotic pathway**
6	Scoparone	10μM or 1μM		Activates constitutive androstane receptor (CAR),activates **xenobiotic pathway**
7	L. Carnitine	10mM or 1μM	Defatting drugs used in our previsous and current studies based on literature reports	Increases **fatty acid transportation** to the mitochondria
8	All-trans Retinoic acid	20μM or 1μM		Activating etinoic acid, **PPAR-β/δ** receptors
9	Coenzyme A	5mM		β-oxidation **substrate**
10	Lipase	50u/mL		Catalyze lipoprotein/TG to into free fatty acid
11	Epigallocatechin gallate (EGCG or E)	0.1μM		Activating AMPK and anti-oxidation/ inflammation
12	Resveratrol (R)	0.5μM		Activating AMPK and SIRT1

Dosages and mechanisms of action of the defatting drugs used in previous (No. 1-6) and current studies (No. 2-12) are listed. The perfusate of control group was supplemented with equal volume of DMSO to the defatting groups; the modified conventional defatting group (Yarmush eg al., Y defatting) was set up as reported (No. 2-10); the second defatting group included the drugs used in Y defatting study, Epigallocatechin gallate (EGCG), and Resveratrol (R) (No. 2-12, Y+E+R defatting). The third defatting group was treated without GW compounds and with dose-reduced defatting drugs (No. 4-12, Y'-GW+E+R defatting).